evidence that E2A overexpression can activate ECs. We have presented evidence clearly demonstrating that E2-2 overexpression inactivates ECs. In addition, E2A alone, like E2-2, blocked VEGFR2-luc reporter activity (supplemental Figure 8B). It is possible that the bilateral activation of ECs by E-proteins is dependent on the presence of other cofactors, such as SCL and LMO2.

Mice lacking the E2-2 gene are initially viable but die within 1 week of birth. No vascular abnormality in E2-2–deficient embryos is observed.[54] It is possible that related genes (E2A and HEB) might compensate for E2-2 gene deficiency during development. If EC-specific knockout mice bearing triple deletions of the E2-2, E2A, and HEB genes can be established, vascular defect(s) might then be seen.

In conclusion, we discovered a novel mechanism by which E2-2 impairs VEGFR2 transcription in ECs. Id1 can overcome the inhibitory effect of E2-2 on VEGFR2 transcription to potentiate EC activation. The identification of compounds that bolster E2-2 activity in an EC-specific manner may provide an exciting opportunity to modulate tumor angiogenesis for therapeutic intervention.

Acknowledgments

The authors thank Dr M. Ema for mouse SCL cDNA, Dr K. Sampath for BMP-6, and Ms F. Miyamasu for excellent English revision.

This work was supported by Grants-in-aid for Scientific Research (17390073, 20012007, 21590328; M.K., S.I.); a Genome Network Project grant (M.K.) from the Japanese Ministry of Education, Culture, Sports, Science and Technology; a Grant-in-Aid for Fellows from the Japan Society for the Promotion of Science (F.I.); the University of Tsukuba Research Project (M.K.); an AstraZeneca Research Grant 2004 (S.I.); the Kowa Life Science Foundation (S.I.); and the Kato Memorial Bioscience Foundation (S.I.).

Authorship

Contribution: A.T. performed most of the research and analyzed the data; F.I. performed the yeast 2-hybrid experiment and critically reviewed the manuscript; K.N. carried out aorta ring assay, interpreted the data, and critically reviewed the manuscript; T.T. contributed to the network formation assay; S.I. designed most aspects of the research, interpreted the data, and drafted the manuscript; and H. K. and M.K. designed parts of the research, interpreted the data, and critically reviewed the manuscript.

Conflict-of-interest disclosure: The authors declare no competing financial interests.

Correspondence: Susumu Itoh, Department of Biochemistry, Showa Pharmaceutical University, 3-3165, Higashi-Tamagawa Gakuen, Machida, Tokyo 194-8543, Japan; e-mail: sitoh@ac.shoyaku.ac.jp.

References

1. Carmeliet P. Angiogenesis in life, disease and medicine. *Nature.* 2005;438(7070):932-936.
2. Adams RH, Alitalo K. Molecular regulation of angiogenesis and lymphangiogenesis. *Nat Rev Mol Cell. Biol.* 2007;8(6):464-478.
3. Perk J, Iavarone A, Benezra R. Id family of helix-loop-helix proteins in cancer. *Nat Rev Cancer.* 2005;5(8):603-614.
4. Lasorella A, Noseda M, Beyna M, Yokota Y, Iavarone A. Id2 is a retinoblastoma protein target and mediates signalling by Myc oncoproteins. *Nature.* 2000;407(6804):592-598.
5. Ohtani N, Zebedee Z, Huot TJ, et al. Opposing effects of Ets and Id proteins on p16INK4a expression during cellular senescence. *Nature.* 2001;409(6823):1067-1070.
6. Benezra R, Davis RL, Lockshon D, Turner DL, Weintraub H. The protein Id: a negative regulator of helix-loop-helix DNA binding proteins. *Cell.* 1990;61(1):49-59.
7. Jen Y, Weintraub H, Benezra R. Overexpression of Id protein inhibits the muscle differentiation program: in vivo association of Id with E2A proteins. *Genes Dev.* 1992;6(8):1466-1479.
8. Langlands K, Yin X, Anand G, Prochownik EV. Differential interactions of Id proteins with basic-helix-loop-helix transcription factors. *J Biol Chem.* 1997;272(32):19785-19793.
9. Ying QL, Nichols J, Chambers I, Smith A. BMP induction of Id proteins suppresses differentiation and sustains embryonic stem cell self-renewal in collaboration with STAT3. *Cell.* 2003;115(3):281-292.
10. Hollnagel A, Oehlmann V, Heymer J, Ruther U, Nordheim A. *Id* genes are direct targets of bone morphogenetic protein induction in embryonic stem cells. *J Biol Chem.* 1999;274(28):19838-19845.
11. Nakashima K, Takizawa T, Ochiai W, et al. BMP2-mediated alteration in the developmental pathway of fetal mouse brain cells from neurogenesis to astrocytogenesis. *Proc Natl Acad Sci U S A.* 2001;98(10):5868-5873.
12. Katagiri T, Yamaguchi A, Komaki M, et al. Bone morphogenetic protein-2 converts the differentiation pathway of C2C12 myoblasts into the osteoblast lineage. *J Cell Biol.* 1994;127(6):1755-1766.
13. Lopez-Rovira T, Chalaux E, Massagué J, Rosa JL, Ventura F. Direct binding of Smad1 and Smad4 to two distinct motifs mediates bone morphogenetic protein-specific transcriptional activation of *Id1* gene. *J Biol Chem.* 2002;277(5):3176-3185.
14. Ogata T, Wozney JM, Benezra R, Noda M. Bone morphogenetic protein 2 transiently enhances expression of a gene, Id (inhibitor of differentiation), encoding a helix-loop-helix molecule in osteoblast-like cells. *Proc Natl Acad Sci U S A.* 1993;90(19):9219-9222.
15. Kowanetz M, Valcourt U, Bergström R, Heldin C-H, Moustakas A. Id2 and Id3 define the potency of cell proliferation and differentiation responses to transforming growth factor β and bone morphogenetic protein. *Mol Cell Biol.* 2004; 24(10):4241-4254.
16. Lyden D, Young AZ, Zagzag D, et al. Id1 and Id3 are required for neurogenesis, angiogenesis and vascularization of tumour xenografts. *Nature.* 1999;401(6754):670-677.
17. Goumans M-J, Valdimarsdottir G, Itoh S, Rosendahl A, Sideras P, ten Dijke P. Balancing the activation state of the endothelium via two distinct TGFβ type I receptors. *EMBO J.* 2002; 21(7):1743-1753.
18. Valdimarsdottir G, Goumans M-J, Rosendahl A, et al. Stimulation of Id1 expression by bone morphogenetic protein is sufficient and necessary for bone morphogenetic protein-induced activation of endothelial cells. *Circulation.* 2002;106(17):2263-2270.
19. Ruzinova MB, Schoer RA, Gerald W, et al. Effect of angiogenesis inhibition by *Id* loss and the contribution of bone-marrow-derived endothelial cells in spontaneous murine tumors. *Cancer Cell.* 2003;4(4):277-289.
20. Itoh F, Itoh S, Goumans M-J, et al. Synergy and antagonism between Notch and BMP receptor signaling pathways in endothelial cells. *EMBO J.* 2004;23(3):541-551.
21. Lazorchak A, Jones ME, Zhuang Y. New insights into E-protein function in lymphocyte development. *Trends Immunol.* 2005;26(6):334-338.
22. Sun XH. Multitasking of helix-loop-helix proteins in lymphopoiesis. *Adv Immunol.* 2004;84:43-77.
23. Murre C. Helix-loop-helix proteins and lymphocyte development. *Nat Immunol.* 2005;6(11): 1079-1086.
24. Einarson MB, Chao MV. Regulation of Id1 and its association with basic helix-loop-helix proteins during nerve growth factor-induced differentiation of PC12 cells. *Mol Cell Biol.* 1995;15(8):4175-4183.
25. Puri PL, Sartorelli V. Regulation of muscle regulatory factors by DNA-binding, interacting proteins, and post-transcriptional modifications. *J Cell Physiol.* 2000;185(2):155-173.
26. Tanaka A, Itoh F, Itoh S, Kato M. TAL1/SCL relieves the E2-2-mediated repression of VEGFR2 promoter activity. *J Biochem.* 2009;145(2):129-135.
27. Ema M, Faloon P, Zhang WJ, et al. Combinatorial effects of *Flk1* and *Tal1* on vascular and hematopoietic development in the mouse. *Genes Dev.* 2003;17(3):380-393.
28. Kawabata M, Inoue H, Hanyu A, Imamura T, Miyazono K. Smad proteins exist as monomers *in vivo* and undergo homo- and hetero-oligomerization upon activation by serine/threonine kinase receptors. *EMBO J.* 1998;17(14):4056-4065.
29. Goldman LA, Cutrone EC, Kotenko SV, Krause CD, Langer JA. Modifications of vectors pEF-BOS, pcDNA1 and pcDNA3 result in improved convenience and expression. *Biotechniques.* 1996;21(6):1013-1015.
30. Sigvardsson M. Overlapping expression of early B-cell factor and basic helix-loop-helix proteins as a mechanism to dictate B-lineage-specific activity of the λ5 promoter. *Mol Cell Biol.* 2000;20(10): 3640-3654.

31. Holderfield MT, Henderson Anderson AM, Kokubo H, et al. HESR1/CHF2 suppresses VEGFR2 transcription independent of binding to E-boxes. *Biochem Biophys Res Commun.* 2006; 346(3):637-648.
32. He T-C, Zhou S, da Costa LT, Yu J, Kinzler KW, Vogelstein B. A simplified system for generating recombinant adenoviruses. *Proc Natl Acad Sci U S A.* 1998;95(5):2509-2514.
33. Takezawa T, Takenouchi T, Imai K, Takahashi T, Hashizume K. Cell culture on thin tissue sections commonly prepared for histopathology. *FASEB J.* 2002;16(13):1847-1849.
34. Itoh F, AsaoH, Sugamura K, Heldin C-H, ten Dijke P, Itoh S. Promoting bone morphogenetic protein signaling through negative regulation of inhibitory Smads. *EMBO J.* 2001;20(15): 4132-4142.
35. Kano MR, Morishita Y, Iwata C, et al. VEGF-A and FGF-2 synergistically promote neoangiogenesis through enhancement of endogenous PDGF-B-PDGFRβ signaling. *J Cell Sci.* 2005; 118(16):3759-3768.
36. Yamada Y, Pannell R, Forster A, Rabbitts TH. The oncogenic LIM-only transcription factor Lmo2 regulates angiogenesis but not vasculogenesis in mice. *Proc Natl Acad Sci U S A.* 2000;97(1):320-324.
37. Lazrak M, Deleuze V, Noel D, et al. The bHLH TAL-1/SCL regulates endothelial cell migration and morphogenesis. *J Cell Sci.* 2004;117(7): 1161-1171.
38. Deleuze V, Chalhoub E, El-Hajj R, et al. TAL-1/SCL and its partners E47 and LMO2 up-regulate VE-cadherin expression in endothelial cells. *Mol Cell Biol.* 2007;27(7):2687-2697.
39. Korchynskyi O, ten Dijke P. Identification and functional characterization of distinct critically important bone morphogenetic protein-specific response elements in the Id1 promoter. *J Biol Chem.* 2002;277(7):4883-4891.
40. Skurk C, Maatz H, Rocnik E, Bialik A, Force T, Walsh K. Glycogen-synthase kinase3β/β-catenin axis promotes angiogenesis through activation of vascular endothelial growth factor signaling in endothelial cells. *Cir Res.* 2005;96(3):308-318.
41. Olsson AK, Dimberg A, Kreuger J, Claesson-Welsh L. VEGF receptor signaling: in control of vascular function. *Nat Rev Mol Cell Biol.* 2006;7(5):359-371.
42. Minami T, Rosenberg RD, Aird WC. Transforming growth factor-β_1-mediated inhibition of the *flk-1/KDR* gene is mediated by a 5′-untranslated region palindromic GATA site. *J Biol Chem.* 2001; 276(7):5395-5402.
43. Zhuang Y, Soriano P, Weintraub H. The helix-loop-helix gene E2A is required for B cell formation. *Cell.* 1994;79(5):875-884.
44. Bain G, Maandag EC, Izon DJ, et al. E2A proteins are required for proper B cell development and initiation of immunoglobulin gene rearrangements. *Cell.* 1994;79(5):885-892.
45. Bain G, Quong MW, Soloff RS, Hedrick SM, Murre C. Thymocyte maturation is regulated by the activity of the helix-loop-helix protein, E47. *J Exp Med.* 1999;190(11):1605-1616.
46. Liu Y, Ray SK, Yang X-Q, Luntz-Leybman V, Chiu I-M. A splice variant of E2-2 basic helix-loop-helix protein represses the brain-specific fibroblast growth factor 1 promoter through the binding to an imperfect E-box. *J Biol Chem.* 1998;273(30): 19269-19276.
47. Markus M, Du Z, Benezra R. Enhancer-specific modulation of E protein activity. *J Biol Chem.* 2002;277(8):6469-6477.
48. Jackson TA, Taylor HE, Sharma D, Desiderio S, Danoff SK. Vascular endothelial growth factor receptor-2: counter-regulation by the transcription factors, TFII-I and TFII-IRD1. *J Biol Chem.* 2005; 280(33):29856-29863.
49. Kappel A, Schlaeger TM, Flamme I, Orkin SH, Risau W, Breier G. Role of SCL/Tal-1, GATA, and Ets transcription factor binding sites for the regulation of *Flk-1* expression during murine vascular development. *Blood.* 2000;96(9):3078-3085.
50. Patterson C, Perrella MA, Hsieh CM, Yoshizumi M, Lee ME, Haber E. Cloning and functional analysis of the promoter for KDR/flk-1, a receptor for vascular endothelial growth factor. *J Biol Chem.* 1995;270(39):23111-23118.
51. Hata Y, Duh E, Zhang K, Robinson GS, Aiello LP. Transcription factors Sp1 and Sp3 alter vascular endothelial growth factor receptor expression through a novel recognition sequence. *J Biol Chem.* 1998;273(30):19294-19303.
52. Illi B, Puri P, Morgante L, Capogrossi MC, Gaetano C. Nuclear factor-κB and cAMP response element binding protein mediate opposite transcriptional effects on the Flk-1/KDR gene promoter. *Circ Res.* 2000;86(12):E110-E117.
53. Nishiyama K, Takaji K, Uchijima Y et al. Protein kinase A-regulated nucleocytoplasmic shuttling of Id1 during angiogenesis. *J Biol Chem.* 2007; 282(23):17200-17209.
54. Zhuang Y, Cheng P, Weintraub H. B-lymphocyte development is regulated by the combined dosage of three basic helix-loop-helix genes, *E2A*, *E2-2* and *HEB*. *Mol Cell Biol.* 1996;16(6):2898-2905.

Inhibition of endothelial cell activation by bHLH protein E2-2 and its impairment of angiogenesis

Supplemental materials for: Tanaka et al

Files in this Data Supplement:

- Document 1. Supplemental methods and figures (PDF, 543 KB)

- Video 1. Time-lapse microscopy of HUVEC network formation: GFP alone (AVI, 536 KB) -
  Forty hours after adenoviral infection, HUVECs were seeded on Matrigels. Ninety minutes later, images were recorded every 15 min by time-lapse microscopy.

- Video 1. Time-lapse microscopy of HUVEC network formation: E2-2 (AVI, 510 KB) -
  Forty hours after adenoviral infection, HUVECs were seeded on Matrigels. Ninety minutes later, images were recorded every 15 min by time-lapse microscopy.

Antibody

Rabbit monoclonal and polyclonal anti-Id1 antibodies were purchased from BioCheck and SantaCruz, respectively. Rabbit monoclonal anti-VEGFR2 or mouse monoclonal anti-E2-2 antibody (M03) was obtained from USBiological and Abnova respectively.

Construct of GFP-HLH

The HLH domain of human E2-2, encompassing from amino acids 577 to 619, was fused to pEGFP-C3 (Clontech).

Electromobility shift assay (EMSA)

EMSA was performed as previously described (1). The double-stranded oligonucleotide consisting of the human VEGFR2 promoter from -40 to +5 (5′ -ttttCCTCCGCGCTCTAGAGTTTCGGCTCCAGCTCCCACCCTGCACTGA-3′ /3′ -aaaaGGAGGCGCGAGATCTCAAAGCCGAGGTCGAGGGTGGGACGTGACT-5′) was end-labeled with [γ-^{32}P]ATP (MP Biochemicals) using T4 polynucleotide kinase (TAKARA). GST proteins and ^{32}P-labeled oligonucleotides were incubated for 30 min at 25°C in binding buffer (20 mM HEPES [pH 7.9], 30 mM KCl, 4 mM $MgCl_2$, 0.1 mM EDTA, 0.8 mM NaPi, 20% glycerol, 4 mM spermidine, 0.3 μg/μl poly(dI·dC), and 0.25 μg/μl salmon sperm DNA) at a final concentration of 30 μl. Protein-DNA complexes were analyzed in 5% nondenaturing polyacrylamide gels containing 0.5× TBE (0.045 M Tris-borate and 0.001 M EDTA [pH 8.0]).

Expresson of GFP in Matrigel plugs

Adenoviruses expressing 1×10^9 pfu of GFP were mixed in the Matrigel solution at 4°C with 200 ng/ml VEGF-A, 1 μg/ml bFGF, and 100 μg/ml heparin. Five hundred microliters of Matrigel containing adenoviruses was injected subcutaneously into the abdomen of male ICR mice. The mice were sacrificed 7 days after the injection. The Matrigel plugs with adjacent subcutaneous tissues were recovered by *en bloc* resection,. Thereafter, each sample was embedded in the OCT compound and quickly frozen in liquid nitrogen to be sectioned at a thickness of 5 μm at -18°C. After being fixed with 4% PFA/PBS, anti-rat monoclonal PECAM-1 antibody (1:200 dilution) was used as a primary antibody. Then, the sections were incubated with Alexa568-conjugated goat anti-rat IgG antibody (1:200 dilution; Molecular Probes). Images were taken using a fluorescence microscope (Zeiss).

Chromatin immunoprecipitation (ChIP) assay

Forty hours after adenoviral infection of HUVECs, HUVECs were treated with 1% formaldehyde in PBS for cross-linking reactions. Cross-linking reactions were stopped by the

addition of PBS-glycine to a final concentration of 0.125 M. Subsequently, the cell lysate was sonicated till the average length of input DNA became less than 500 bp in size. Then, the control IgG or anti-Myc9E10 antibody was used for the immunoprecipitation. After purification of immunoprecipitated DNAs, Primers specific for detection of the VEGFR2 promoter including the imperfect E2-2 binding site were used for amplification of DNA fragments. Primers used here were 5′ -GTAAATGGGCTTGGGGAGCT-3′ and 5′ -AAACGCAGCGACCACACACT-3′ .

REFERENCES

1. Itoh S, Ericsson J, Nishikawa J, Heldin CH, ten Dijke P. The transcriptional co-activator P/CAF potentiates TGF-β/Smad signaling. *Nucleic. Acids. Res.* 2000; 28:4291–4298.

Figure S1. Interaction of E2-2 with Id1 in ECs

Endogenous interaction between Id1 and E2-2. MEECs were stimulated with BMP6 for 3 h. Total lysates were equally divided into two experiments for Fig. 1c and Suppl. Fig. 1. Immunoprecipitation was performed with an anti-Id1 polyclonal antibody, followed by western blotting with an anti-E2-2 monoclonal antibody (upper panel). The arrow indicates the band corresponding to E2-2. Expression of Id1 in immunoprecipitates was checked using an anti-Id1 polyclonal antibody (lower panel). Expression of E2-2 and Id1 in total lysates was shown in Fig. 1c. As a negative control, the rabbit control IgG was used for immunoprecipitation.

Figure S2. Requirement of the HLH domains for Id1 and E2-2 to interact with each other

(A) Structure of E2-2ΔHLH and Id1ΔHLH constructs. (B) E2-2 requires its HLH domain for homodimer formation. The experiment was performed in a similar manner to that described in Figure 1a. Detection of E2-2 homodimer (upper panel). Expression of Myc-E2-2 was evaluated with an anti-Myc 9E10 antibody (middle panel). Flag-E2-2 and Flag-E2-2ΔHLH were detected using an anti-Flag M5 antibody (lower panel). (C) Id1 requires its HLH domain to interact with E2-2. The experiment was performed as described in Figure 1a. Heterodimer formation between Id1 and E2-2 (upper panel). Expression of Myc-E2-2 using an anti-Myc 9E10 antibody (middle panel). Flag-Id1 and Flag-Id1ΔHLH levels were shown using an anti-Flag M5 antibody (lower panel). (D) E2-2 requires its HLH domain to interact with Id1. The experiment was performed as described in Figure 1a. Id1 coimmunoprecipitated with E2-2 (upper panel). Expression of Myc-Id1 using an anti-Myc 9E10 antibody (middle panel). Expression of Flag-E2-2 and Flag-E2-2ΔHLH was shown using an anti-Flag M5 antibody (lower panel). (E) The HLH domain in E2-2 is enough for E2-2 to interact with Id1. Myc-Id1 was co-transfected with either

GFP or GFP-HLH in COS7 cell. The experiment was performed as described in Figure 1a. GFP-HLH/Id1 heterodimer formation is shown in the upper panel. Expressions of Myc-Id1 (middle panel), and GFP or GFP-HLH (lower panel) were evaluated using an anti-Myc 9E10 and anti-GFP antibodies, respectively.

Figure S3. Effect of E2-2 on the activities of MCKpfos-luc and pGL2b-VEGFR2-luc (-166bp/+267bp)

(A) E2-2 potentiates MCKpfos-luc activity. MEECs were transfected with MCKpfos-luc and different amounts of E2-2. (B) Id1 inhibits E2-2-induced MCKpfos-luc activity. MEECs were transfected with MCKpfos-luc and different amounts of Id1 (1 and 5 pg) and E2-2. (C) pGL2b-VEGFR2-luc (-166bp/+267bp) activity is suppressed by E2-2. MEECs were transfected with pGL2b-VEGFR2-luc (-166bp/+267bp) and different amounts of E2-2.

Figure S4. Expression of GFP in endothelial cells in the Matrigel plugs

The sections in Fig. 4b were observed with a fluorescence microscopy. Since GFP was co-expressed with E2-2 by the adenoviral gene transfer, we examined whether GFP was expressed in PECAM-1-positive endothelial cells (red). Arrows indicate GFP-positive endothelial cells, whereas the arrowhead shows GFP-negative endothelial cells.

Figure S5. Effect of E2-2 on EC's function

(A) Expression of EC markers in calf pulmonary aortic endothelial cells (CPAEs). Total RNA was prepared from CPAEs or bovine aortic endothelial cells (BAEC)s. Amplified products are indicated on the left of the figure. GAPDH mRNA was analyzed as an internal control. BAECs were used as known ECs from bovines. Primer sets used here are shown in Supplemental Table II. (B) Expression of VEGFR2 protein in HUVECs expressing E2-2. Forty hours after adenoviral infection, cell lysates were prepared and analyzed by western blotting using indicated antibodies. The expression of VEGFR2 protein was normalized with that of β-actin protein. Each relative intensity was calculated by the comparison of the intensity of the band corresponding to VEGFR2 proteins in HUVECS without E2-2- and Id1-adenoviral gene tranfer. (C) Effect of E2-2 on cell proliferation. HUVECs were infected with either GFP- or E2-2-expressing adenovirueses. Five days after infection, we measured cell growth using Cell Titer 96®Aqueous One Solution Reagent (Promega).

Figure S6. Disruption of E2-2-DNA complex by Id1

(A) Direct binding of E2-2 to the VEGFR2 promoter. *E. coli*-expressed GST fusion proteins were incubated with a ^{32}P-labeled probe. (lane1) probe alone; (lane 2) GST alone; (lane 3)

GST-E2-2; (lane 4) GST-E2-2 plus GST-Id1; (lane 5) GST-Id1. A specific complex of GST-E2-2 with the labeled probe is indicated by an arrow. Each relative intensity was calculated by the comparison of the intensity of the shifted band (arrow) in lane 3. (B) Dissociation of E2-2 from the VEGFR2 promoter by Id1. HUVECs were infected with E2-2- and/or Id1-expressing adenoviruese. After 40 hours of infection, the sonicated chromatin-protein complex was immunoprecipitated with either control IgG or anti-Myc-9E10 antibody. Immunoprecipitated DNAs with control IgG (upper panel) and anti-Myc9E10 antibodies (2nd panel) were isolated and then amplified using primers specific to VEGFR2 promoter including the imperfect E2-2 binding site. The 3rd panel reveals total chromatin before immunoprecipitation as an input. Expression of E2-2 and Id1 in HUVECs was detected using anti-Myc9E10 (4^{th} panel) and anti-Id1 antibodies (lower panel), respectively.

Figure S7. Function of E2A

(A) Id1 inhibits E2A-induced MCKpfos-luc activity. MEECs were transfected with MCKpfos-luc and different amounts of E2A and Id1. (B) E2A inhibits pGL2b-VEGFR2-luc (-166bp/+267bp) activity. MEECs were transfected with pGL2b-VEGFR2-luc (-166bp/+268bp) and E2A. (C) Id1 interacts with E2A and E2-2. Myc-Id1 was cotransfected with Flag-E2A or Flag-E2-2. Immnunoprecipitations were carried out using an anti-Flag M5 antibody, and coimmunoprecipitated Id1 was detected by western blotting using an anti-Myc9E10 antibody (upper panel). The expression of Myc-Id1 and proteins conjugated with Flag at N-terminus were blotted on the membrane and probed with an anti-Myc9E10 antibody (middle panel) and an anti-Flag M5 antibody (lower panel), respectively.

Figure S8. Model of regulation of VEGFR2 promoter by E2-2

In the steady state, E2-2 binds to the VEGFR2 promoter together with other transcription factor(s) (termed X) to block transcription of VEGFR2 gene. When the expression of Id1 is induced, Id1 interacts with E2-2 via an HLH domain interaction, thereby removing E2-2 from the promoter and activating transcription of VEGFR2 gene.

Figure S1

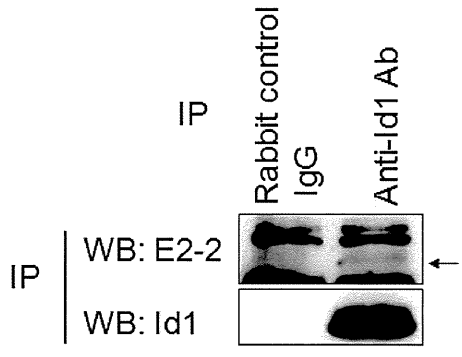

Figure S2

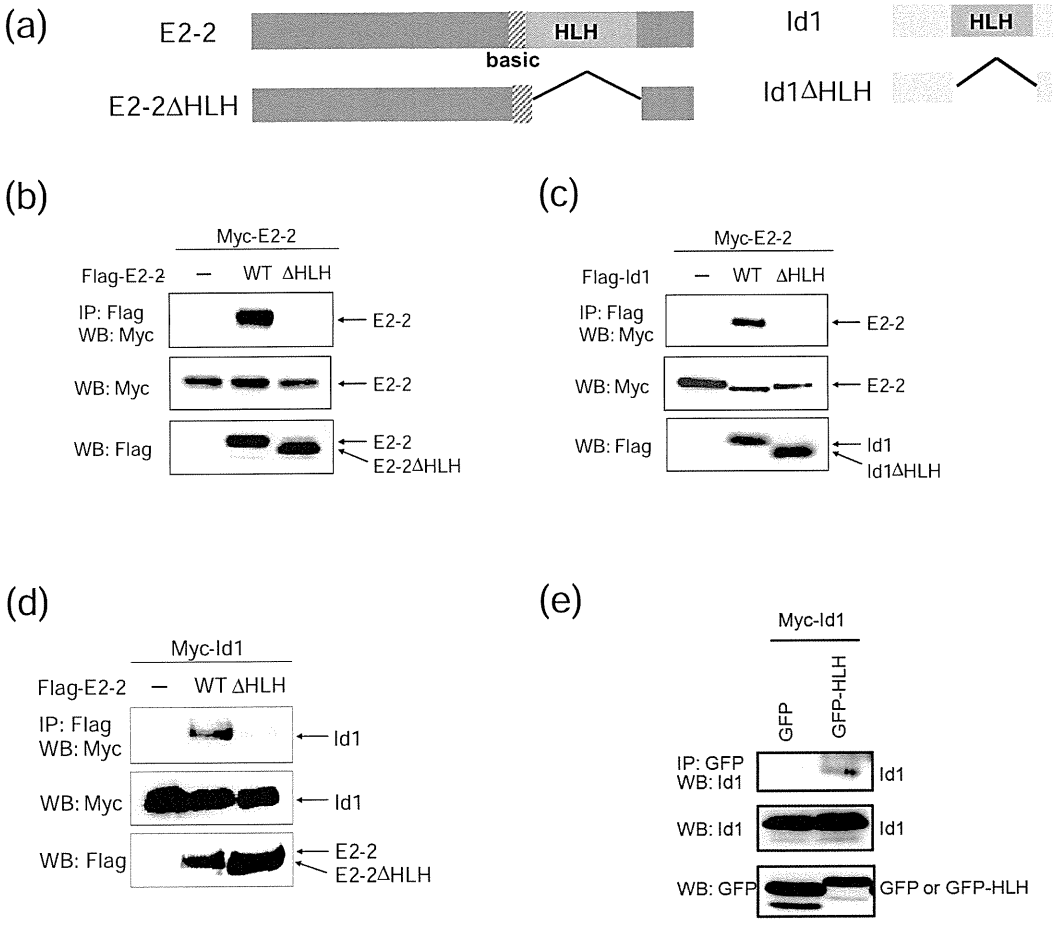
(a)
E2-2
HLH
basic
E2-2ΔHLH
Id1
HLH
Id1ΔHLH
(b)
Myc-E2-2
Flag-E2-2
–
WT
ΔHLH
IP: Flag
WB: Myc
E2-2
WB: Myc
E2-2
WB: Flag
E2-2
E2-2ΔHLH
(c)
Myc-E2-2
Flag-Id1
–
WT
ΔHLH
IP: Flag
WB: Myc
E2-2
WB: Myc
E2-2
WB: Flag
Id1
Id1ΔHLH
(d)
Myc-Id1
Flag-E2-2
–
WT
ΔHLH
IP: Flag
WB: Myc
Id1
WB: Myc
Id1
WB: Flag
E2-2
E2-2ΔHLH
(e)
Myc-Id1
GFP
GFP-HLH
IP: GFP
WB: Id1
Id1
WB: Id1
Id1
WB: GFP
GFP or GFP-HLH

Figure S3

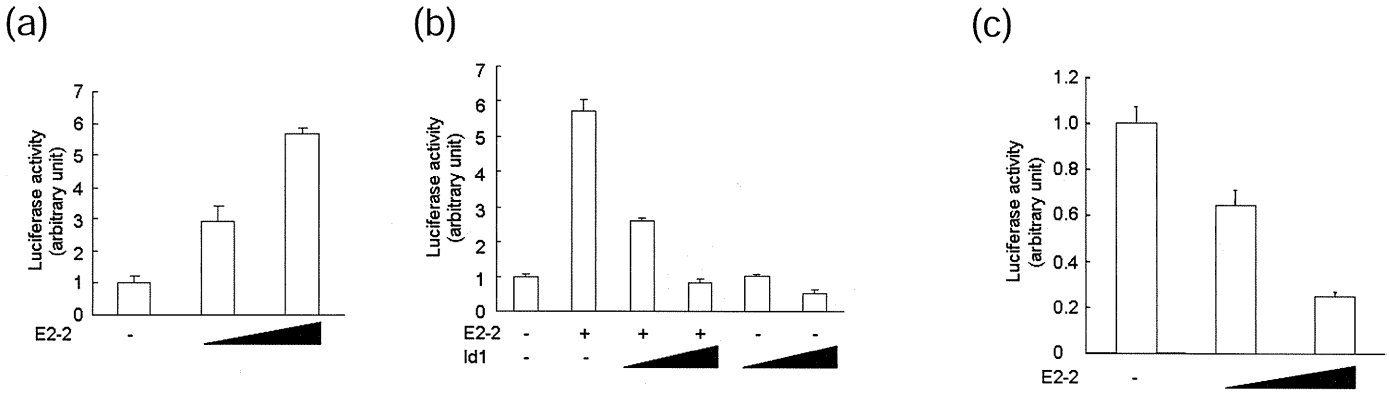
(a)
Luciferase activity (arbitrary unit)
0
1
2
3
4
5
6
7
E2-2
-
(b)
Luciferase activity (arbitrary unit)
0
1
2
3
4
5
6
7
E2-2 - + + + - -
Id1 - -
(c)
Luciferase activity (arbitrary unit)
0
0.2
0.4
0.6
0.8
1.0
1.2
E2-2
-

Figure S4

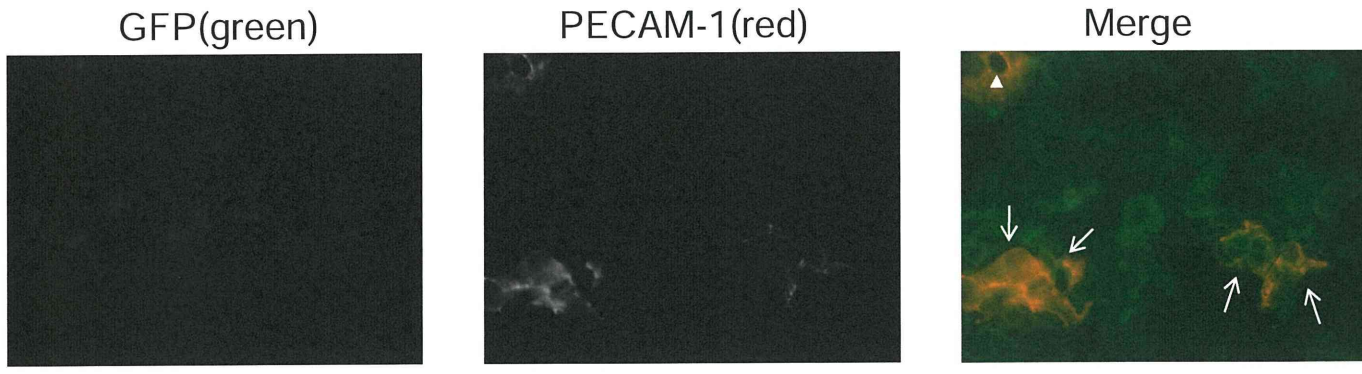

Figure S5

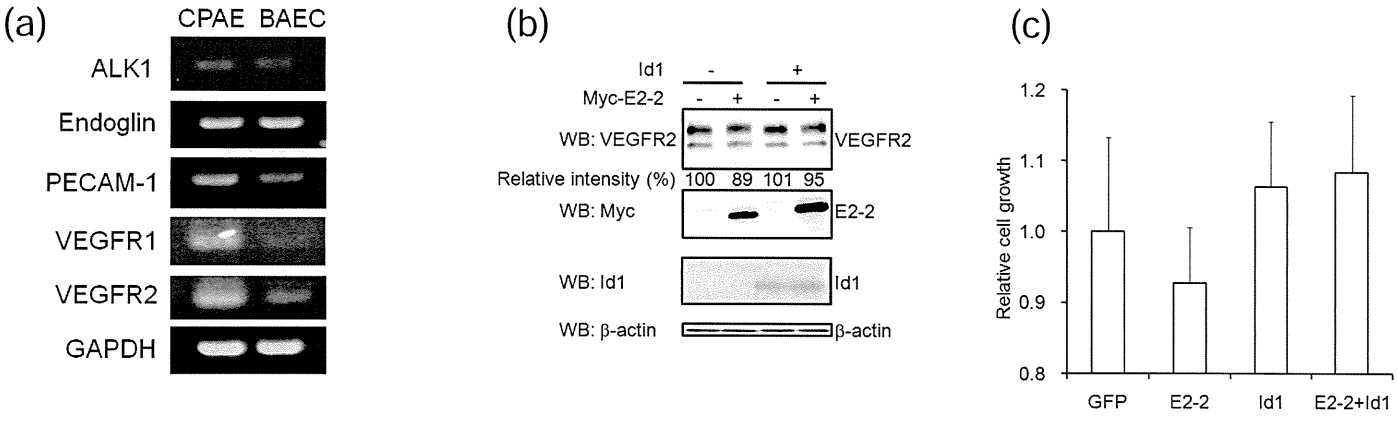
(a)
CPAE
BAEC
ALK1
Endoglin
PECAM-1
VEGFR1
VEGFR2
GAPDH
(b)
Id1
Myc-E2-2
WB: VEGFR2
VEGFR2
Relative intensity (%) 100 89 101 95
WB: Myc
E2-2
WB: Id1
Id1
WB: β-actin
β-actin
(c)
Relative cell growth
1.2
1.1
1.0
0.9
0.8
GFP
E2-2
Id1
E2-2+Id1

Figure S6

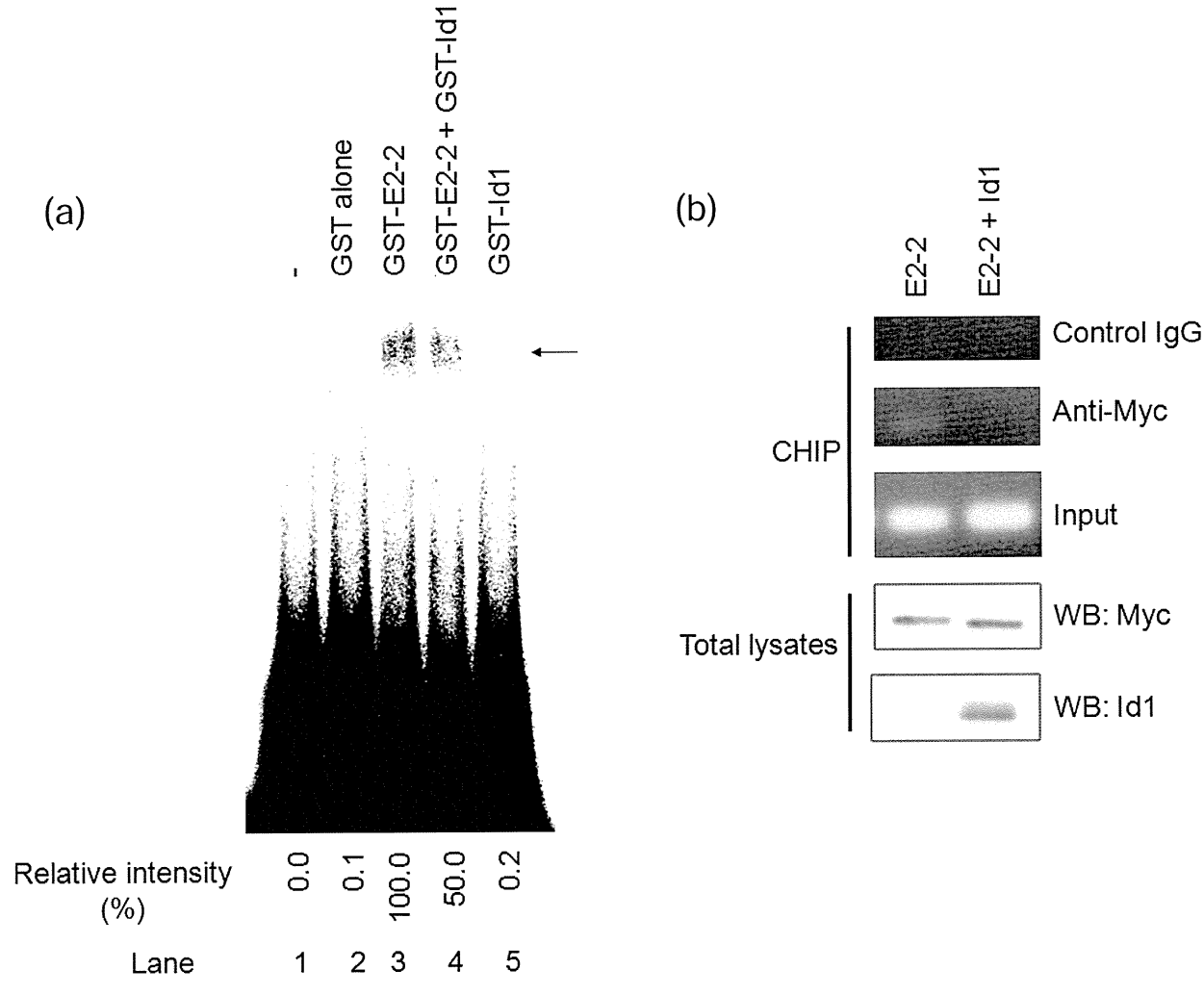
(a)
-
GST alone
GST-E2-2
GST-E2-2 + GST-Id1
GST-Id1
Relative intensity (%)
0.0
0.1
100.0
50.0
0.2
Lane
1
2
3
4
5
(b)
E2-2
E2-2 + Id1
CHIP
Control IgG
Anti-Myc
Input
Total lysates
WB: Myc
WB: Id1

Figure S7

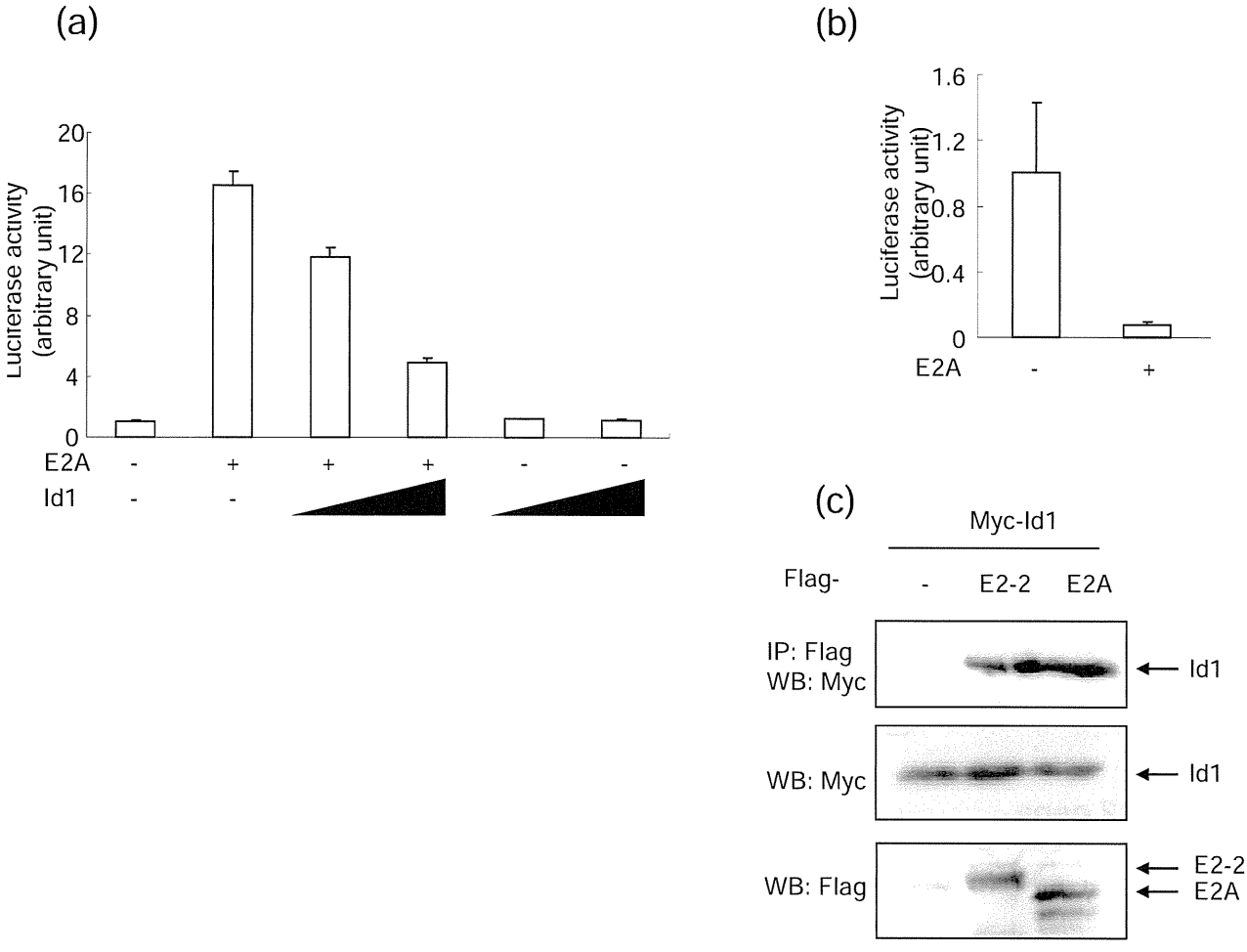
(a)
Luciferase activity (arbitrary unit)
20
16
12
8
4
0
E2A - + + + - -
Id1 - - ▲ ▲
(b)
Luciferase activity (arbitrary unit)
1.6
1.2
0.8
0.4
0
E2A - +
(c)
Myc-Id1
Flag- - E2-2 E2A
IP: Flag
WB: Myc
Id1
WB: Myc
Id1
WB: Flag
E2-2
E2A

Figure S8

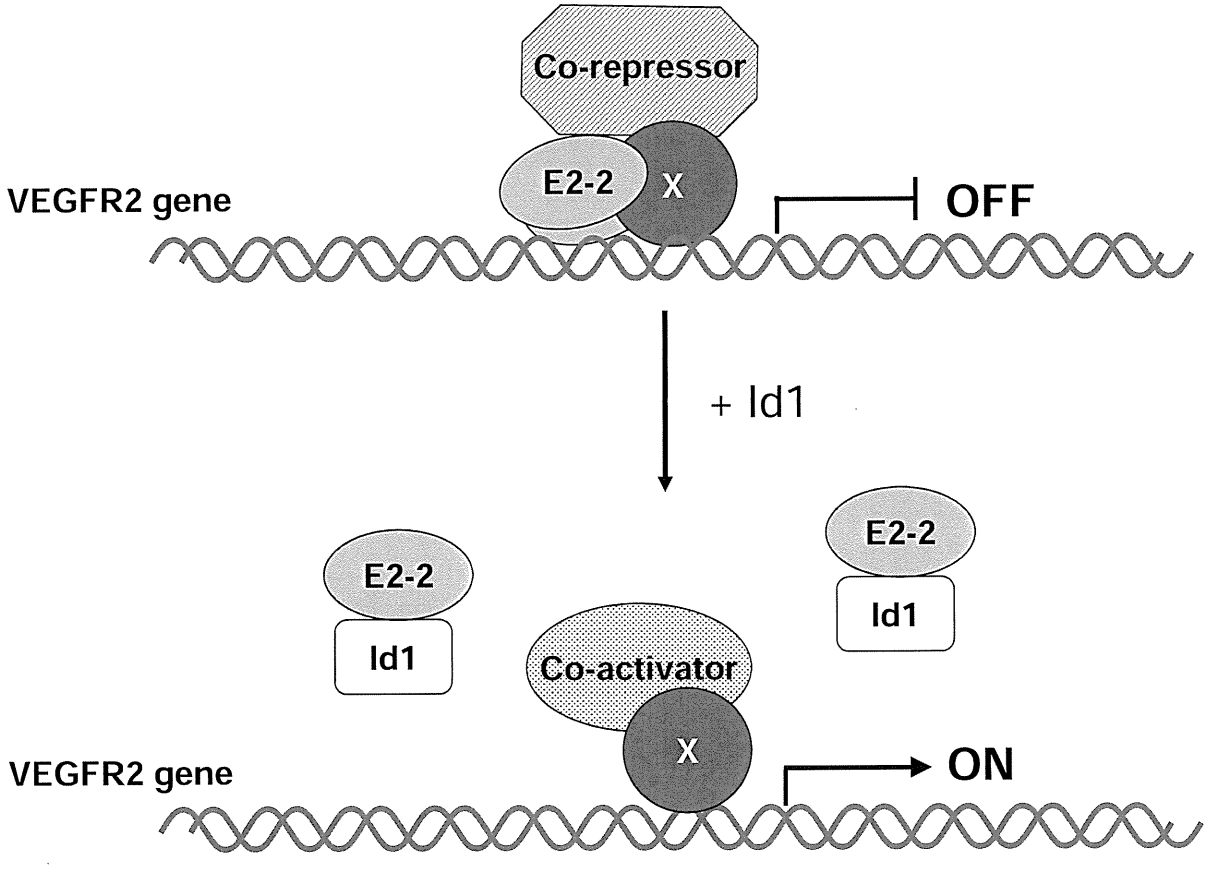
Co-repressor
E2-2
X
VEGFR2 gene
OFF
+ Id1
E2-2
Id1
E2-2
Id1
Co-activator
X
VEGFR2 gene
ON

Calcitonin gene-related peptide facilitates revascularization during hindlimb ischemia in mice

Toshiaki Mishima, Yoshiya Ito, Kanako Hosono, Yukio Tamura, Yasushi Uchida, Mitsuhiro Hirata, Tatsunori Suzsuki, Hideki Amano, Shintaro Kato, Yukiko Kurihara, Hiroki Kurihara, Izumi Hayashi, Masahiko Watanabe and Masataka Majima

Am J Physiol Heart Circ Physiol 300:H431-H439, 2011. First published 3 December 2010; doi:10.1152/ajpheart.00466.2010

AJP - Heart and Circulatory Physiology publishes original investigations on the physiology of the heart, blood vessels, and lymphatics, including experimental and theoretical studies of cardiovascular function at all levels of organization ranging from the intact animal to the cellular, subcellular, and molecular levels. It is published 12 times a year (monthly) by the American Physiological Society, 9650 Rockville Pike, Bethesda MD 20814-3991. ISSN: 0363-6135, ESSN: 1522-1539. Visit our website at http://www.the-aps.org/.

Am J Physiol Heart Circ Physiol 300: H431–H439, 2011.
First published December 3, 2010; doi:10.1152/ajpheart.00466.2010.

Calcitonin gene-related peptide facilitates revascularization during hindlimb ischemia in mice

Toshiaki Mishima,[1,2] Yoshiya Ito,[1] Kanako Hosono,[2] Yukio Tamura,[1] Yasushi Uchida,[1] Mitsuhiro Hirata,[1] Tatsunori Suzsuki,[2] Hideki Amano,[3] Shintaro Kato,[4] Yukiko Kurihara,[5] Hiroki Kurihara,[5] Izumi Hayashi,[6] Masahiko Watanabe,[1] and Masataka Majima[2]

Departments of [1]Surgery, [2]Pharmacology, [3]Thoracic Surgery, and [4]Cardio-angiology, Kitasato University School of Medicine, Kanagawa; [5]Department of Physiological Chemistry and Metabolism, Graduate School of Medicine, Tokyo University, Tokyo; and [6]Faculty of Pharmaceutical Sciences, Department of Pathophysiology, Nippon Pharmaceutical University, Saitama, Japan

Submitted 14 May 2010; accepted in final form 1 December 2010

Mishima T, Ito Y, Hosono K, Tamura Y, Uchida Y, Hirata M, Suzsuki T, Amano H, Kato S, Kurihara Y, Kurihara H, Hayashi I, Watanabe M, Majima M. Calcitonin gene-related peptide facilitates revascularization during hindlimb ischemia in mice. *Am J Physiol Heart Circ Physiol* 300: H431–H439, 2011. First published December 3, 2010; doi:10.1152/ajpheart.00466.2010.—It is known that the neural system plays a fundamental role in neovascularization. A neuropeptide, calcitonin gene-related peptide (CGRP), is widely distributed in the central and peripheral neuronal systems. However, it remains to be elucidated the role of CGRP in angiogenesis during ischemia. The present study examined whether endogenous CGRP released from neuronal systems facilitates revascularization in response to ischemia using CGRP knockout mice ($CGRP^{-/-}$). $CGRP^{-/-}$ or their wild-type littermates ($CGRP^{+/+}$) were subjected to unilateral hindlimb ischemia. $CGRP^{-/-}$ exhibited impaired blood flow recovery from ischemia and decreased capillary density expressed in terms of the number of CD-31-positive cells in the ischemic tissues compared with $CGRP^{+/+}$. In vivo microscopic studies showed that the functional capillary density in $CGRP^{-/-}$ was reduced. Hindlimb ischemia increased the expression of pro-CGRP mRNA and of CGRP protein in the lumbar dorsal root ganglia. Lack of CGRP decreased mRNA expression of growth factors, including CD31, vascular endothelial growth factor-A, basic fibroblast growth factor, and transforming growth factor-β, in the ischemic limb tissue. The application of CGRP enhanced the mRNA expression of CD31 and VEGF-A in human umbilical vein endothelial cells (HUVECs) and fibroblasts. Subcutaneous infusion of CGRP8–37, a CGRP antagonist, using miniosmotic pumps delayed angiogenesis and reduced the expression of proangiogenic growth factors during hindlimb ischemia. These results indicate that endogenous CGRP facilitates angiogenesis in response to ischemia. Targeting CGRP may provide a promising approach for controlling angiogenesis related to pathophysiological conditions.

neuropeptide; sensory nerve; ganglia

PROGNOSIS OF PATIENTS WITH acute lower ischemia still remains poor. The formation of new blood vessels in response to ischemia is an important adaptive response that preserves tissue integrity and is regulated by hypoxia and inflammation (8). New blood vessels grow postnatally by means of angiogenesis [i.e., capillary sprouting of resident endothelial cells (ECs)], arteriogenesis, and vasculogenesis (i.e., de novo vascularization from EC precursors) but also grow in adults (8). It is widely known that the neuronal system plays a fundamental role in the maturation of primitive embryonic vasculature. Mutations that disrupt peripheral sensory nerves or Schwann cells prevent proper arteriogenesis, whereas those that disorganize the nerves maintain the alignment of arteries with misrouted axons (24). Sensory neurons have been shown to modulate the expression of arterial markers on ECs via the secretion of vascular endothelial growth factor (VEGF) (23).

Primary afferent sensory neurons transmit sensory information from peripheral tissues to the spinal cord and brain. The cell bodies of the sensory nerve fibers that innervate the head and body are located in the trigeminal ganglia and dorsal root ganglia (DRG) and can be divided into two main categories, namely myelinated A-fibers and unmyelinated C-fibers. These sensory fibers are specialized sensory neurons known as nociceptors, which detect environmental stimuli. Nociceptors express a diverse repertoire of receptors and transduction molecules that can sense forms of noxious stimulation (i.e., thermal, mechanical, and chemical stimulation) with varying degrees of sensitivity (21). Nociceptor activation results in the release of neurotransmitters, such as calcitonin gene-related peptide (CGRP), endothelin, histamine, glutamate, and substance P (21).

CGRP is a 37-amino acid neuropeptide produced in DRG by tissue-specific alternative splicing of the primary transcript of the calcitonin/CGRP gene (3). CGRP is widely distributed in the central and peripheral neuronal systems and exhibits numerous biological activities, including responses to sensory stimuli, cardiovascular regulation, and vasodilation (3, 6, 15). Endogenous CGRP has been shown to protect the heart (16) against ischemic injury and damage. We have reported that CGRP plays critical roles in the maintenance of gastric mucosal integrity (4, 5, 28). Maintenance of gastric mucosal integrity is highly dependent on the alarm systems that can rapidly sense the harmful chemical or mechanical stimuli to which the mucosa is exposed. The gastrointestinal tract is known to be rich in neuronal systems, among which afferent neurons of extrinsic origin are reported to operate as an emergency protective system (15). The functions of these afferents sensitive to chemicals are reported to be mediated by CGRP released in the gastric mucosa (28).

It was reported that one of the sensory neuropeptides, substance P, has a proangiogenic activity (10); however, the details of the mechanism underlying enhanced angiogenesis were not precisely studied. It was reported that CGRP stimulates the proliferation of cultured human umbilical vein endo-

Address for reprint requests and other correspondence: M. Majima, Dept. of Pharmacology, Kitasato Univ. School of Medicine, 1-15-1 Kitasato, Minami-ku, Sagamihara, Kanagawa, 252-0374, Japan (e-mail: mmajima@med.kitasato-u.ac.jp).

thelial cells (HUVECs) (14). In addition, we recently found that CGRP has a proangiogenic activity. CGRP enhances tube formation activity in a coculture system using HUVECs and fibroblasts (29). Moreover, endogenous CGRP promotes tumor growth and tumor-associated angiogenesis (29). These observations suggest that CGRP would be involved in the regulation of angiogenesis; however, little is known about the role of CGRP in the revascularization in response to acute ischemia in vivo. Thus the present study was conducted to investigate the roles of CGRP in blood flow recovery and angiogenesis during unilateral hindlimb ischemia using CGRP gene-disrupted mice (26).

MATERIALS AND METHODS

Animals. Male C57BL/6 mice (8 wk of age) were obtained from CLEA Japan (Tokyo, Japan). A strain of male CGRP knockout mice ($CGRP^{-/-}$, 8 wk of age) developed by us (26) and their wild-type littermates ($CGRP^{+/+}$) were used. All mice were maintained at a constant humidity (60 ± 5%) and temperature (25 ± 1°C) and kept continuously on a 12:12-h light-dark cycle. All procedures conducted on animals were performed in accordance with the guidelines for animal experimentation of Kitasato University School of Medicine. The study protocol was approved by the Animal Care and Use Committee (2076, 2010–125).

Model of acute hindlimb ischemia. Hindlimb ischemia was induced as described elsewhere (2, 17). Under anesthesia with pentobarbital sodium (50 mg/kg ip), a midline incision was made in the abdominal skin, which permitted dissection to expose the external iliac artery and vein in the upper part of the left limb. The artery and vein were then ligated both proximally and distally using 6–0 silk suture, and the intervening 6-mm section was excised. Next, the incision was closed.

Continuous administration of a CGRP antagonist, CGRP8–37. A CGRP antagonist, CGRP8–37 (Peptide Institute, Osaka, Japan), in the physiological saline was infused in the subcutaneous tissues at a rate of 50 nmol/day using osmotic pumps (Azlet; DURECT, Cupertino, CA). The delivery rate was 0.5 μl/h, and the mice received CGRP8–37 for 14 days. One day after the implantation of pumps, mice were subjected to hindlimb ischemia. Mice treated with vehicle (physiological saline) served as controls.

Laser doppler flow analysis. Blood flow to the right and left hindlimbs was assessed by scanning the lower abdomen and limbs of the mice with a laser Doppler blood flowmeter (Laser Doppler Perfusion Imager System, moorLDI-Mark 2; Moor Instruments, Wilmington, DE), as previously reported (2, 17). The ratio of blood flow in the ischemic (left) to the nonischemic (right) limb was calculated by dividing the integrated blood flow in an area of the image that included the left foot pad by the integrated blood flow in an area of the same size that included the right foot pad.

Measurement of blood pressure and heart rate. The mean arterial blood pressure (MAP) and heart rate (HR) in conscious mice were determined by a programmable sphygmomanometer (BP-98A; Softron, Tokyo, Japan) using the tail-cuff method as reported previously (17).

Immunohistochemistry. Immunostaining was performed with the use of CD31 (1:100 dilution; Santa Cruz Biotechnology, Santa Cruz, CA) or CGRP (1:100 dilution; Enzo Life Sciences, Plymouth Meeting, PA), as reported previously (17). For quantification, the numbers of CD31-positive cells were counted in 10 randomly selected transverse sections in each animal. The results were averaged, and capillary density was expressed in terms of the number of CD31-positive cells per high-power field.

In vivo microscopy. Seven days after surgery, animals were anesthetized with pentobarbital sodium (50 mg/kg ip) and were prepared for in vivo fluorescence microscopy as previously described (17, 19). The hindlimb microcirculation was observed using a fluorescence microscope (ECLIPSE E600, upright type; Nikon) with a 100-W mercury lamp for epi-illumination. The microscopic images were obtained with a long-working-distance objective lens (M plan 40/0.40 SLWD; Nikon) and a ×10 eyepiece lens. Images of the microcirculation were transmitted through a charge-coupled device camera (C7190; Hamamatsu Photonics; Hamamatsu) to a television monitor screen (PVM-144Q; Sony) and were recorded for subsequent off-line analysis on videotape with an S-VHS recorder (BR-S600; Victor). Plasma was labeled with 1 mg/ml iv of fluorescein isothiocyanate-dextran (Sigma) just before the observation. Microcirculation in the quadriceps muscles (muscular regions) or through the tissues adjacent to the femoral artery and vein (perifemoral regions) was observed.

Analysis of in vivo microscopy. To evaluate the blood flow through the capillaries in the ischemic limb, the total length of perfused capillaries per observation area was measured and expressed as functional capillary density (mm/mm^2). The functional capillary density was determined in 10 different perifemoral and muscular regions in each animal.

Isolation of lumbar DRG neurons. Under ether anesthesia, the medulla spinalis was removed, and the lumbar DRG neurons of the L_1-L_5 levels were dissected from the spinal cord.

Real-time RT-PCR. Transcripts encoding CD31, VEGF-A, basic fibroblast growth factor (bFGF), transforming growth factor-β (TGF-β), pro-CGRP, and glyceraldehyde-3-phosphate dehydrogenase (GAPDH) were quantified by real-time RT-PCR analysis as described previously (17). Total RNA was extracted from the ischemic muscle tissues or DRG using TRIzol (GIBCO), and single-stranded cDNA was generated from 1 μg of total RNA via reverse transcription using ReverTra Ace-α (TOYOBO). Quantitative PCR amplification was performed using SYBR Premix Ex Taq (Takara Bio) and the following gene-specific primers: for CD31, 5′-CCCTTCATTGACCTCAACTACAATGGT-3′(sense) and 5′-GAGGGGCCATCCACAGTCTTCTG-3′ (antisense); for VEGF, 5′-CCCCAGAATGAAGGTTACACA-3′ (sense) and 5′-TGTCAAAGGGAGAAGGGTTTT-3′ (antisense); for bFGF, 5′-CCCCAGAAAATGAAGGTTACACA- 3′ (sense) and 5′-TGTCAAACCGAAGGAGAAGGGTTTT-3′ (antisense); for TGF-β, 5′-CCCCAGAATGAAGGGTTACACA- 3′ (sense) and 5′-TGTCAAAGGGAGAAAGGGTTTT-3′ (antisense); for pro-CGRP, 5′-CCCCAGAATGAAGGTTACACA-3′ (sense) and 5′-TGTCAAAGGGAGAAGGGTTTT-3′ (antisense); and, for GAPDH, 5′-CCCTTCATTGACCTCCAACTACAATGGT-3′ (sense) and 5′-GAGGGGCCATCCACACGTCTTCTG-3′ (antisense).

RT-PCR analysis in HUVECs and fibroblasts. HUVECs purchased from Kurabo (Tokyo, Japan) were cultured in 10% FBS and endothelial cell growth supplement (EGM-2 MV; Cambrex Bioscience, Wekerville, MD). Confluent HUVEC (incubated in serum-free media) were treated with CGRP (3 and 30 μM) and PBS for 6 h. Next, HUVECs were collected and homogenized with Trizol (Invitrogen, Carlsbad, CA). Murine fibroblasts (L929) were obtained from Cell Bank, RIKEN Bioresource Center (Ibaraki, Japan). They were cultured in DMEM supplemented with 10% (vol/vol) FBS and 100 U/500 ml penicillin, all of which were obtained from GIBCO-BRL, Life Technologies (Rockville, MD), at 37°C in 5% humidified CO_2 as reported elsewhere (18). L929 fibroblasts (3×10^5 cells/well) were incubated for 6 h with CGRP (3 and 30 μM) and PBS. We tested the mRNA expression of VEGF-A and CD31 in HUVECs and fibroblasts by real-time RT-PCR.

We also tested the mRNA expression of the following CGRP receptors: calcitonin receptor-like receptor (CRLR) (a subunit of CGRP1), calcitonin receptor (CTR) a (a subunit of CGRP2), and receptor activity-modifying protein (RAMP)−1 (a common subunit of CGRP receptor) in HUVECs and fibroblasts by real-time RT-PCR. The primers used for HUVECs were as follows: for CRLR, 5′-AACAACCAGGCCTTAGTAGCC-3′ (sense) and 5′-CCTTCACAGAGCATCCAAAAG-3′ (antisense); for CTRa, 5′-GCTTGGCACTGTTTCTTCTTC-3′ (sense) and 5′-CATCCATCATCTTCTTTCGTC-3′ (antisense); for RAMP-1, 5′-TCACCTCTTCATGACCACACTGC-3′ (sense) and 5′-TCCCTG-

TAGCTCCTGATGGTC-3′ (antisense); and for GAPDH, 5′-CAACTTTGGTATCGTGGAAGG-3′ (sense) and 5′-AGAGGCAGGGATGATGTTCTG-3′ (antisense). The primers used for L929 fibroblasts were as follows: for CRLR, 5′-CTTCTGGATGCTCTGTGAAGG-3′ (sense) and 5′-CCCAGCCGAGAAAATAATACC-3′ (antisense); for CTRa, 5′-GAACTGTCACCACCCTTACCC-3′ (sense) and 5′-TCGCAGAGCATCCAGAAGTAG-3′ (antisense); for RAMP-1, 5′-CCATCTCTTCATGGTCACTGC-3′ (sense) and 5′-AGCGTCTTCCCAATAGTCTCC-3′ (antisense); and for GAPDH, 5′-ACATCAAGAAGGTGGTGAAGC-3′ (sense) and 5′-AAGGTGGAAGAGTGGGAGTTG-3′ (antisense).

Statistics. All data were expressed as means ± SE. Multiple comparisons were performed using one-way ANOVA with a post hoc Fisher's test. The statistical difference between the two groups was examined using Student's unpaired *t*-test after confirming that the variance of data was not heterogeneous. Differences were considered to be significant for P values of <0.05.

RESULTS

Impaired angiogenesis during hindlimb ischemia in CGRP knockout mice. To examine the role of CGRP in neovascularization, blood flow recovery was assessed by laser Doppler flowmetry in ischemic and nonischemic limbs after femoral ligation in $CGRP^{-/-}$ and $CGRP^{+/+}$. Figure 1*A* shows representative images of hindlimb blood flow recorded before and after surgical induction of ischemia. The ratio of blood flow in ischemic to nonischemic hindlimbs was similar in the two groups of mice before surgery (Fig. 1*B*). Immediately after surgery, hindlimb blood flow was severely reduced in both strains, to the same extent, indicating that the severity of ischemia was comparable. In $CGRP^{+/+}$, hindlimb blood flow gradually recovered to ~77% of the levels of the nonischemic limb over the next 14 days. In contrast, the blood flow recovery was impaired in $CGRP^{-/-}$ compared with $CGRP^{+/+}$ (Fig. 1*B*). Ischemic/nonischemic limb blood flow ratios in $CGRP^{-/-}$ were 28% (*day 3*), 40% (*day 7*), and 14% (*day 14*) less than in $CGRP^{+/+}$. At 21 days after surgery, the levels of blood flow recovery in $CGRP^{+/+}$ and $CGRP^{-/-}$ were restored to 78 and 74%, respectively, compared with baseline levels. There was no difference in blood flow levels between the two groups. Figure 1*C* demonstrates photomicrographs of representative ischemic limb sections stained with an antibody against CD31 at 7 days after surgery. Quantitative analysis revealed that capillary density expressed in terms of the number of CD31-

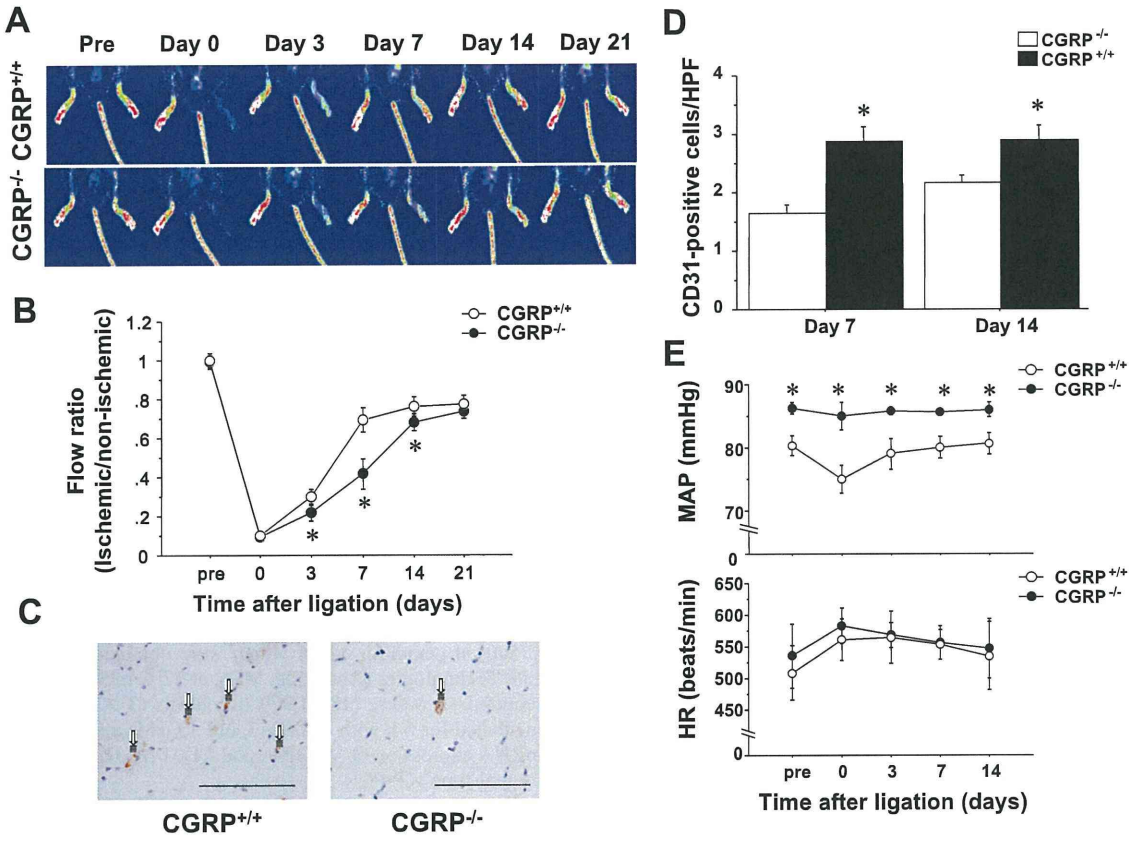

Fig. 1. Impaired blood flow recovery and angiogenesis during hindlimb ischemia in calcitonin gene-related peptide (CGRP) knockout mice. Hindlimb ischemia was induced in CGRP knockout mice ($CGRP^{-/-}$) and in their wild-type littermates ($CGRP^{+/+}$). *A*: representative laser Doppler flowmetry (LDF) images recorded before (pre), immediately after (0), and 3, 7, 14, and 21 days after surgical induction of hindlimb ischemia in $CGRP^{-/-}$ and $CGRP^{+/+}$. *B*: time course of ischemic/nonischemic blood flow ratios in $CGRP^{-/-}$ and $CGRP^{+/+}$. Results are expressed as a ratio in the left (ischemic) to right (nonischemic) limb. Data are means ± SE from 6 mice/group. $^*P < 0.05$ vs. $CGRP^{+/+}$. *C*: photographs of ischemic muscle sections stained with an anti-CD31 antibody from $CGRP^{+/+}$ (*left*) and $CGRP^{-/-}$ (*right*) 7 days after the hindlimb ischemia. Bars indicate 100 μm. *D*: quantitative analysis of capillary density expressed in terms of the no. of CD-31-positive cells/high-power field (HPF) 7 and 14 days after the hindlimb ischemia. Data are expressed as means ± SE from 6 mice/group. $^*P < 0.05$ vs. $CGRP^{-/-}$. *E*: changes in mean arterial blood pressure (MAP) and heart rate (HR) before and after surgery. Data are expressed as means ± SE from 6 mice/group. $^*P < 0.05$ vs. $CGRP^{+/+}$.

positive cells per field in CGRP$^{-/-}$ 7 days after surgery was significantly reduced by 46% compared with that in CGRP$^{+/+}$ (Fig. 1*D*). At 14 days after surgery, capillary density in CGRP$^{-/-}$ was still lower (25% reduction) than that in CGRP$^{+/+}$ (Fig. 1*D*), although the difference between the two groups at 14 days was smaller than that at 7 days. We also measured MAP and HR in conscious mice. MAPs in CGRP$^{-/-}$ were higher than those in WT, although there was no significant difference in HRs between the two groups throughout the experiments (Fig. 1*E*).

We observed the microcirculation through the tissue adjacent to the femoral artery and vein (perifemoral regions) or in the quadriceps muscles (muscular regions) 7 days after surgery (Fig. 2). Higher-magnification images of in vivo fluorescence microscopy demonstrated that revascularization in the perifemoral and in the muscular regions was suppressed in CGRP$^{-/-}$ (Fig. 3*A*). Quantitative analysis revealed that the functional capillary density in the perifemoral and muscular regions was reduced (by 46 and 44%, respectively) in CGRP$^{-/-}$ compared with that in CGRP$^{+/+}$ (Fig. 3*B*).

These results suggested that endogenous CGRP plays a role in blood flow recovery and angiogenesis during hindlimb ischemia.

Increased pro-CGRP expression in the lumbar DRG during hindlimb ischemia. To estimate the increase in CGRP release during ischemia-induced angiogenesis, we determined the mRNA levels of pro-CGRP, a precursor of CGRP, in DRG (L_1-L_5). Hindlimb ischemia caused increased pro-CGRP expression in the ipsilateral lumbar DRG 1, 3, and 7 days after surgery by 19, 32, and 15%, respectively compared with sham-operated mice (Fig. 4*A*). Expression of pro-CGRP returned to normal levels by 14 days after surgery. These results suggested that hindlimb ischemia upregulated pro-CGRP in the DRG, which innervated the area of ischemia.

We assessed the immunoreactivity with CGRP in the DRG during hindlimb ischemia (Fig. 4*B*). The enhanced CGRP-expressing DRG neurons together with numerous CGPR-immunoreactive nerve fibers were shown 3 days after the induction of ischemia compared with sham operation. Next, the immunoreactivity with CGRP was attenuated at 7 days. In addition, enhanced CGRP immunoreactivity in CGRP$^{+/+}$ was demonstrated on peripheral nerves distributed in the ischemic muscles (Fig. 4*C*, *top*) of the ischemic limbs 7 days after ischemia compared with CGRP$^{-/-}$ (Fig. 4*C*, *bottom*).

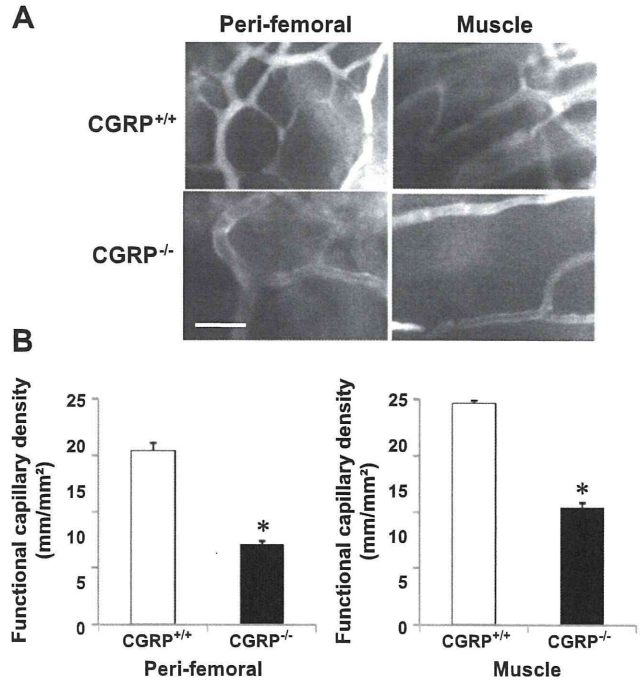

Fig. 3. Hindlimb microcirculation in response to ischemia. *A*: representative in vivo micrographs of ischemic limbs 7 days after the induction of surgical ischemia in CGRP$^{-/-}$ and CGRP$^{+/+}$. Revascularization in the tissues along the femoral vessels (perifemoral regions) and in the muscular regions was impaired in CGRP$^{-/-}$ compared with CGRP$^{+/+}$. Scale bar indicates 20 μm. *B*: functional capillary density in the perifemoral and muscular regions in ischemic limbs was determined 7 days after the surgical induction of ischemia. Data are means ± SE from 6 mice/group. *$P < 0.05$ vs. CGRP$^{+/+}$.

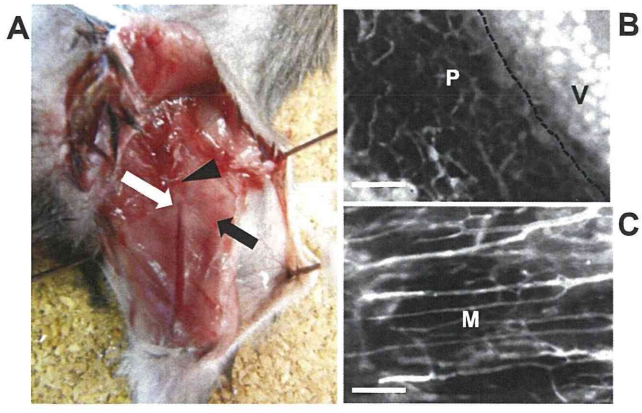

Fig. 2. Surgical preparation for in vivo microscopy. Hindlimb ischemia was elicited by the ligation of the left femoral artery and vein (black arrowhead). *A*: surgical preparation for in vivo microscopic studies was performed as described in MATERIALS AND METHODS. The tissue along the femoral vessels (white arrow) and muscle tissue (black arrow) were observed. *B* and *C*: representative in vivo fluorescence micrographs of the hindlimb microcirculation 7 days after the induction of ischemia. The microvasculature adjacent to the femoral vein (perifemoral regions) (*B*) and in the muscle tissue (muscular regions) (*C*) was visualized by the injection of fluorescein isothiocyanate (FITC)-dextran. V, femoral vein; P, perifemoral tissue; M, muscle tissue. Bar indicates 100 μm.

Downregulated expression of proangiogenic factors in CGRP$^{-/-}$ mice. Because angiogenesis is affected by proangiogenic factors, we determined the levels of mRNA expression of angiogenic factors in the ischemic tissues 3 and 7 days after surgery, by real-time RT-PCR analysis. The mRNA expression of proangiogenic factors, including CD31 (60 and 40%) (Fig. 5*A*), VEGF-A (28 and 44%) (Fig. 5*B*), bFGF (38 and 32%) (Fig. 5*C*), and TGF-β (64 and 39%) (Fig. 5*D*), in the ischemic tissues of CGRP$^{-/-}$ was significantly reduced compared with that of CGRP$^{+/+}$.

Upregulated expression of proangiogneic factors in HUVECs and fibroblasts treated with CGRP. To elucidate the contribution of CGRP to angiogenesis, HUVECs and fibroblasts were cultured in the presence of CGRP. We found that CGRP at final concentrations of 30 μM enhanced the mRNA expression of CD31 (Fig. 6*A*) and VEGF-A (Fig. 6*B*) in HUVECs. In addition, VEGF-A mRNA expression in L929 fibroblasts was upregulated (Fig. 6*C*).

Furthermore, we tested mRNA expression of the CGRP receptors CRLR, CTRa, and RAMP-1 in HUVECs and fibro-